

## Soft Swimming: Exploiting Deformable Interfaces for Low Reynolds Number Locomotion

Renaud Trouilloud,<sup>1</sup> Tony S. Yu,<sup>1</sup> A. E. Hosoi,<sup>1</sup> and Eric Lauga<sup>2,\*</sup>

<sup>1</sup>*Hatsopoulos Microfluids Laboratory, Department of Mechanical Engineering, Massachusetts Institute of Technology, 77 Massachusetts Avenue, Cambridge, Massachusetts 02139, USA*

<sup>2</sup>*Department of Mechanical and Aerospace Engineering, University of California San Diego, 9500 Gillman Drive, La Jolla California 92093-0411, USA*

(Received 15 January 2008; published 24 July 2008)

Reciprocal movement cannot be used for locomotion at low Reynolds number in an infinite fluid or near a rigid surface. Here we show that this limitation is relaxed for a body performing reciprocal motions near a deformable interface. Using physical arguments and scaling relationships, we show that the nonlinearities arising from reciprocal flow-induced interfacial deformation rectify the periodic motion of the swimmer, leading to locomotion. Such a strategy can be used to move toward, away from, and parallel to any deformable interface as long as the length scales involved are smaller than intrinsic scales, which we identify. A macroscale experiment of flapping motion near a free surface illustrates this new result.

DOI: 10.1103/PhysRevLett.101.048102

PACS numbers: 47.63.Gd, 47.15.G–, 47.55.N–

Swimming microorganisms inhabit a world quite different from the one we experience. Their motion through the surrounding fluid occurs at very low Reynolds numbers (Re), a fact with two important consequences: (a) the only physical force available to produce thrust is drag; (b) since the fluid equations (Stokes equations) are linear and time-reversible, swimming motions symmetric with respect to time reversal (reciprocal motion) cannot be used for locomotion (the scallop theorem [1]). Biological swimmers, such as bacteria and spermatozoa, overcome these two limitations by exploiting the anisotropic drag of slender filaments such as flagella and cilia, and actuating these filaments in a wavelike fashion [2,3].

Motivated by the recent development of artificial swimmers [4], we pose here the following general question: are there any new low-Re swimming methods remaining to be discovered? In particular, can some simple reciprocal movements produce locomotion, thereby apparently violating the constraints of the scallop theorem?

In this Letter, we propose a new method for locomotion without inertia. Using theory and experiments, we show that a body performing a reciprocal movement is able to move near a soft interface: physically, the deformation of the interface provides the geometric nonlinearities necessary to escape the constraints of the scallop theorem. This strategy, which is relevant for sufficiently small systems, also implies that the time-reversible component of all swimmers (including biological organisms) can generate nontrivial flows and propulsive forces near soft interfaces.

The physical picture for soft swimming arises from the asymmetries between different modes of motion near deformable interfaces, and can be illustrated by considering the motion of a rigid sphere slowly translating below a free surface (Fig. 1). For motion perpendicular to the interface, the drag on the sphere is always increased by the presence of the interface; however, the magnitude and direction of the surface-induced component of the drag can be modulated by deforming the interface [5,6]. When the sphere

moves away from the interface [Fig. 1(a)], it displaces fluid with it, and the interface deforms toward the sphere, resulting in an increase of the surface-induced drag,  $F_{\text{down}} > F_{\text{flat}}$ . In contrast, when the sphere moves toward the interface [Fig. 1(b)], the free surface is displaced away from the sphere, and the component of the drag due to the interface is diminished,  $F_{\text{up}} < F_{\text{flat}}$ . The asymmetry,  $\Delta F = F_{\text{down}} - F_{\text{up}} > 0$ , results in an averaged net force on the fluid,  $\Delta F$ , away from the interface if the sphere is oscillated in a reciprocal fashion. (Alternatively, if the sphere is acted upon by an external force with zero average, it will move toward the interface.) For motion parallel to the interface [Figs. 1(c) and 1(d)], surface deformation leads to a lift force on the sphere, perpendicular to its direction of motion and directed away from the interface [7,8], reminiscent of the lift force responsible for the migration of deformable bodies such as droplets [9], vesicles [10,11], and polymers [12] away from boundaries. These effects are due to the nonlinear (geometric) coupling between the moving sphere and the deformable interface, and they vanish when the interfaces do not deform. A similar coupling can be exploited for locomotion.

Let us consider a body—a swimmer—that deforms in a prescribed and periodic fashion. On length scales larger than the typical size of the swimmer, the disturbance flow field can be modeled as a superposition of point flow

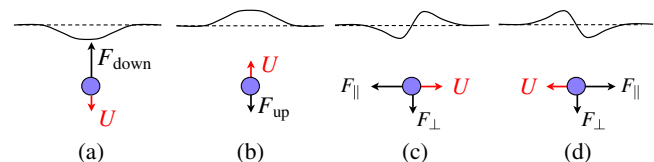


FIG. 1 (color online). Breakdown of reversibility near soft interfaces: a sphere moving away from a soft surface experiences more drag than one moving toward the interface,  $F_{\text{down}} > F_{\text{up}}$  (a),(b); a sphere translating parallel to a soft surface experiences a lift force,  $F_{\perp}$ , perpendicular to the direction of motion (c),(d).

disturbances. Since a low-Re swimmer cannot exert any net force on the surrounding fluid, the instantaneous velocity field decays at most like a force dipole [Fig. 2(a)]; the swimmer is also torque free, and therefore only symmetric force dipoles are allowed (stresslets [13,14]). In three dimensions, the dipole strength  $\mathbf{p}$  is a 3-by-3 tensor with 6 independent components. The associated flow field decays as  $\sim 1/r^2$  and is given by  $\mathbf{u}^p = \frac{p_{ij}}{8\pi\eta r^3}(-\delta_{ij} + 3\frac{x_i x_j}{r^2})\mathbf{r}$ , where  $\eta$  is the fluid viscosity, and  $\mathbf{r} = x_i \mathbf{e}_i$  is the distance to the dipole. There exist two types of dipoles: parallel dipoles, in which the direction of the forces is aligned with that of the force gradient [Fig. 2(b)], and perpendicular dipoles, in which these directions are perpendicular to one another [Fig. 2(c)]. Furthermore, in general, the flow field can contain other types of singularities (higher moments of force distribution), with faster spatial decay, predominantly the potential (source) dipole [Fig. 2(d)], of vector strength  $\mathbf{q}$ , associated with a velocity field decaying as  $\sim 1/r^3$  and given by  $u_i^q = \frac{q_j}{8\pi\eta r^3}(-\delta_{ij} + 3\frac{x_i x_j}{r^2})$ .

In an infinite fluid, and by linearity of Stokes equations, the velocity of a swimmer whose far field is described by a superposition of stresslets and potential dipoles is given by  $\mathbf{u} = \mathbf{M} \cdot \mathbf{p} + \mathbf{N} \cdot \mathbf{q}$ , where the mobility matrices  $\mathbf{M}$  and  $\mathbf{N}$  are functions of the instantaneous shape of the swimmer; here, we will take  $\mathbf{M}$  and  $\mathbf{N}$  as constants, a suitable approximation for bodies performing small-amplitude swimming motions. We also consider swimmers with sufficiently symmetric motion so that their orientation remains constant and ignore torque balance.

We now examine the case of a swimmer located near an undeformable interface. The presence of the interface will result in additional velocity for the swimmer,  $\mathbf{u}_w(h)$ , where  $h$  is the distance to the interface, due to the image singu-

larities required to enforce the correct boundary conditions at the interface [15]. The equation for the swimming velocity becomes  $\mathbf{u} = \mathbf{M} \cdot \mathbf{p} + \mathbf{N} \cdot \mathbf{q} + \mathbf{u}_w(h)$ , where the wall-induced velocity is given by  $\mathbf{u}_w(h) = \frac{1}{32\pi\eta h^2}[(p_{xx} + p_{zz} - 2p_{yy})\mathbf{e}_y - \frac{1}{2h}(q_x \mathbf{e}_x + q_z \mathbf{e}_z + 2q_y \mathbf{e}_y)]$  in the case of a flat free surface [illustrated by the dashed arrows in Figs. 2(e)–2(g)]; results for no-slip surfaces are similar. Note that the magnitude of  $\mathbf{u}_w(h)$  scales linearly with the dipole strengths  $\mathbf{p}$  and  $\mathbf{q}$ . In general, surfaces of fixed shape will lead to an equation for the swimming kinematics given by  $\frac{d\mathbf{x}}{dt} = \mathbf{A}(\mathbf{r}) \cdot \mathbf{p}(t) + \mathbf{B}(\mathbf{r}) \cdot \mathbf{q}(t)$ . For reciprocal deformations, we have  $\mathbf{p}(t) = \mathbf{p}_0 f(t)$ ,  $\mathbf{q}(t) = \mathbf{q}_0 f(t)$ , where  $f$  is an arbitrary periodic function of time: the swimming kinematics are described by an autonomous dynamical system, and no locomotion can occur on average,  $\langle \mathbf{u} \rangle = 0$ . This is the scallop theorem.

We now consider interfaces that can deform due to the flow set up by the swimmer. Since wall effects depend on the shape of, and the distance to the interface, and since both can be modified by the swimmer's flow field, the relationship between the local reciprocal actuation and the swimming kinematics becomes nonlinear.

Let us consider a free surface, with surface tension  $\gamma$ , and show that motion toward, away from, and parallel to the surface can be devised. For motion toward the surface, we only need to consider parallel force dipoles aligned with the surface,  $\mathbf{p} = p(t)\mathbf{e}_x \mathbf{e}_x$  [Figs. 2(h) and 2(i)]. We assume small Capillary number to capture the first-order effect of surface deformation ( $p/\gamma h^2 \ll 1$ ). The normal deformation of the interface (magnitude  $\delta$ ) is set by the balance between capillary and viscous forces at the interface,  $\gamma\delta/h^2 \sim -p/h^3$ , hence  $\delta \sim -p/\gamma h$ ; note that the surface deformation can be calculated analytically for small Capillary numbers, as plotted in Figs. 2(h)–2(l). The wall-induced velocity on the dipole, due to the image system, now has a magnitude  $u_w = \mathbf{e}_y \cdot \mathbf{u}_w \sim p/\eta(h + \delta)^2$ , and can be linearized around  $h_0$  (the starting position of the swimmer) to obtain  $u_w \sim p/\eta(h_0)^2 - p\delta/\eta h_0^3 \sim p/\eta(h_0)^2 + p^2/\gamma\eta h_0^4$ . The swimming kinematics in the  $y$  direction are then given by  $dh/dt \sim Mp(t) + p(t)^2/\gamma\eta h_0^4 - p(t)/\eta h_0^2$ . For reciprocal swimming  $p(t) = p_0 \cos\omega t$ , we get a net locomotion toward the surface, with average swimming velocity  $\langle u_y \rangle \sim p_0^2/\gamma\eta h_0^4$  [16]. In practice, the dipole arises from the unsteady actuation of a swimmer of size  $L$  with velocity  $U \sim \omega L$ , and therefore  $p_0 \sim \eta L^2 U$ , so that  $\langle u_y \rangle/U \sim (\eta U/\gamma)(L/h_0)^4$ : for sufficiently large deformations  $\eta U/\gamma \sim 1$  and confined swimmers  $L/h_0 \sim 1$ , we obtain a net speed on the order of the actuation speed  $\langle u_y \rangle \sim U$  [17].

The physical interpretation for this motion toward the surface is illustrated in Figs. 2(h) and 2(i). When  $p > 0$ , the swimmer deflects the surface toward it, enhancing the wall-induced attraction [Fig. 2(h), dashed arrow] by a small amount (empty arrow); when  $p < 0$ , the surface is deflected away from the swimmer, reducing the wall-induced repulsion [Fig. 2(i), dashed arrow], by a small amount

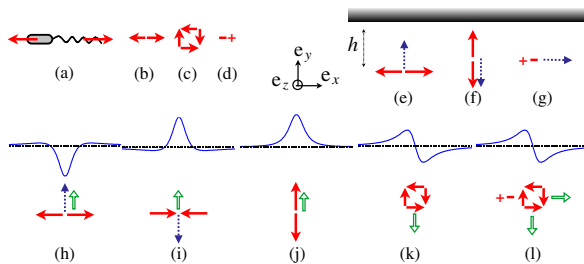


FIG. 2 (color online). Physics of soft swimming. (a) The lowest-order flow around a low-Re swimmer decays as a force dipole; (b) parallel force dipole ( $p_{xx} > 0$ ); (c) perpendicular force dipole ( $p_{xy} < 0$ ); (d) potential (source) dipole ( $q_x > 0$ ); (e)  $p_{xx} > 0$  is attracted by a flat surface; (f)  $p_{yy} > 0$  is repelled by a flat surface; (g)  $q_x < 0$  moves parallel to a flat surface; (h)  $p_{xx} > 0$  deforms a soft surface in a manner that enhances the attraction; (i)  $p_{xx} < 0$  deforms the same surface in a manner that reduces the repulsion; (j) a reciprocal  $p_{yy}$  is attracted by a soft surface; (k) a reciprocal  $p_{xy}$  is repelled by a soft surface; (l) a reciprocal combination of  $p_{xy}$  and  $q_x$  moves away from, and parallel to a deformable surface.

(empty arrow). Both deformation-induced effects are directed toward the surface, and therefore do not average to zero for a reciprocal actuation. The results are similar for a parallel force dipole in the direction perpendicular to the surface,  $\mathbf{p} = p(t)\mathbf{e}_y\mathbf{e}_y$  [Fig. 2(j)].

Locomotion away from the surface can be obtained by considering perpendicular force dipoles, of the form  $\mathbf{p} = p(t)(\mathbf{e}_x\mathbf{e}_y + \mathbf{e}_y\mathbf{e}_x)$  [Fig. 2(k)]. In that case, the surface deformation is asymmetric, and it induces a lift force which does not average to zero with  $p$  [5]. The scaling for the time-averaged swimming speed is similar to the previous section, except that it is now directed away from the free surface  $\langle u_y \rangle \sim -p_0^2/\gamma\eta h_0^4$ .

Moving parallel to the deformable surface is more subtle. Indeed, since the first effect of surface deformation is always directed perpendicular to the undisturbed surface [5], the only way to move parallel to the surface is to use motion toward or away from the surface to rectify an otherwise time-periodic and spatially dependent parallel motion [such as the one illustrated in Fig. 2(g)]. This can be achieved, for example, by combining a perpendicular force dipole,  $\mathbf{p} = p(t)(\mathbf{e}_x\mathbf{e}_y + \mathbf{e}_y\mathbf{e}_x)$ , with a potential dipole,  $\mathbf{q} = q(t)\mathbf{e}_x$  [Fig. 2(l)]. Since the flow field due to the potential dipole decays faster (by 1 order of magnitude) than that due to the force dipole, the first effect of surface deformation will be the establishment of the lift force due to  $p$ . The swimming kinematics are therefore given by  $dh/dt \sim -p(t)^2/\gamma\eta h^4$  in the direction perpendicular to the surface, and  $dx/dt \sim -q(t)/\eta h^3$  in the parallel direction. Writing  $h(t) = h_0 + \tilde{h}(t)$ , with  $\tilde{h}(t) \ll h_0$ , we have  $dx/dt \sim -q/\eta h_0^3 + q\tilde{h}/\eta h_0^4$ . For a reciprocal motion with  $p(t) = p_0 \cos(\omega t + \varphi)$  and  $q(t) = q_0 \cos(\omega t + \varphi)$ , time integration leads to  $\tilde{h}(t) = -p_0^2(t + \sin(2\omega t + 2\varphi)/2\omega)/\gamma\eta h_0^4$ , and therefore the average swimming speed in the  $x$  direction is given by  $\langle u_x \rangle \sim -p_0^2 q_0 \sin\varphi/\omega\gamma\eta^2 h_0^8$ . Thus swimming occurs both away from the surface and in the  $+x$  or  $-x$  direction, depending on the sign of  $\sin\varphi$ . Similarly, combining a force dipole in the  $\mathbf{e}_x\mathbf{e}_x$  or  $\mathbf{e}_y\mathbf{e}_y$  direction with a source dipole along  $\mathbf{e}_x$  leads to combined motion toward and parallel to the surface.

The examples above demonstrate that a free surface can be exploited to obtain locomotion in all directions using reciprocal forcing. To analyze the effectiveness of these swimming strategies, three types of biologically relevant soft surfaces can be considered (Fig. 3): the interface between two liquids [Fig. 3(a)], an elastic membrane separating two liquids [Fig. 3(b)], and the interface between a liquid and an elastic gel [Fig. 3(c)].

Consider a fluid with viscosity  $\eta$  and density  $\rho$ , in which all length scales  $L$  (swimmer size  $a$ , distance to the surface  $h$ ) are similar. For soft swimming to occur, the local reciprocal actuation of the swimmer has to generate flow speeds  $U$  sufficiently small for the Reynolds number,  $\text{Re} = \rho UL/\eta$ , to be small, yet large enough to induce significant deformation of the interface, i.e., a large (a) capillary number,  $\text{Ca} = \eta U/\gamma$ , for the interface between two fluids

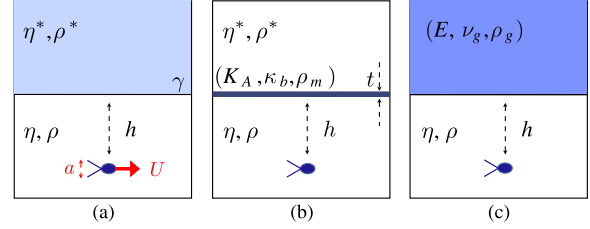


FIG. 3 (color online). Examples where soft swimming can occur: (a) interface between two liquids (or between a liquid and a gas), (b) elastic membrane separating two liquids, and (c) interface between a liquid and an elastic gel (see text for notation).

with similar viscosities ( $\eta$ ,  $\eta^*$ ) and densities ( $\rho$ ,  $\rho^*$ ), (b) dimensionless membrane-viscous number,  $\text{Me} = \eta U/K_A$ , for two fluids separated by an elastic membrane (thickness  $t$ , area modulus  $K_A$ , density  $\rho_m$ , bending stiffness  $\kappa_B$ ), (c) elastoviscous number,  $\text{El} = \eta U/LE$ , for an elastic gel (Young's modulus  $E$ , Poisson's ratio  $\nu_g$ , density  $\rho_g$ ). By combining  $\text{Re} < 1$  with (a)  $\text{Ca} > 1$ , (b)  $\text{Me} > 1$ , (c)  $\text{El} > 1$ , we find that soft swimming is expected to be effective for length scales below (a)  $L < \ell_f$ , where  $\ell_f = \eta^2/\rho\gamma$  is an intrinsic viscocapillary length scale (the Ohnesorge length), (b)  $L < \ell_m$ , where  $\ell_m = \eta^2/\rho K_A$  is the intrinsic membrane-viscous length scale, (c)  $L < \ell_g$ , where  $\ell_g = \sqrt{\eta^2/\rho E}$  is the intrinsic elastoviscous length scale [18].

To examine the biological relevance of these ideas, we consider an environment where motility is crucial, namely, the female reproductive tract in humans [19]. In this case, the fluids involved (e.g. cervical mucus) have viscosities in the range  $\eta \sim 0.1\text{--}10$  Pa s [20], leading to values of  $\ell_f$  between fractions of millimeters to meters. A similar range for  $\ell_m$  is obtained in the case where such fluids are separated by a lipid bilayer [21], and for  $\ell_g$  when the fluids are near an elastic gel such as a crosslinked actin network [21]. In all cases, the intrinsic length scales are large, and therefore biological flows arising from time-reversible motion could be substantial.

To further illustrate the breaking of the scallop theorem near soft surfaces, we exploit the increase of the intrinsic scale  $\ell_f$  with the viscosity, and perform a macroscale experiment near a free surface. Instead of a swimmer, we consider a flapper fixed in place, for which the problem of reciprocal swimming is replaced by the dual problem of reciprocal pumping, i.e., creating a nonzero flow from a time-periodic forcing.

A thin plate, the flapper (size  $2\text{ cm} \times 7\text{ cm}$ ), was mounted to the shaft of a servomotor and rotated over a range of  $90^\circ$  ( $45^\circ$  on each side) at flapping periods of  $3\text{--}200$  s [Fig. 4(a)]. The flapper was immersed in a high-viscosity silicone oil ( $\eta = 60$  Pa s,  $\ell_f \approx 50$  m) with the tip of the flapper positioned  $2$  cm below the free surface; alternatively, the free surface could be covered by a solid acrylic sheet to prevent surface deformation. A laser sheet

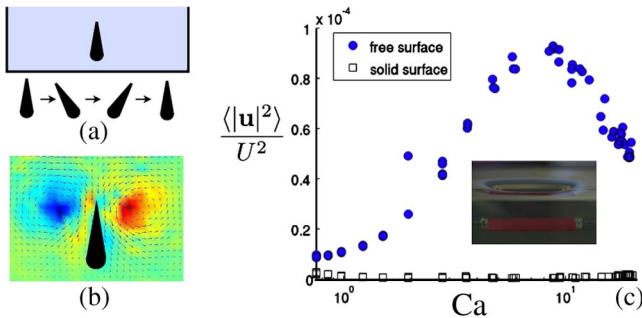


FIG. 4 (color online). Experiment to generate a net flow by reciprocal flapping motion below a free surface; (a) principle of the experiment; (b) velocity and vorticity fields over one flapping cycle (top right is positive vorticity); (c) dimensionless kinetic energy over one cycle as a function of the flapping capillary number,  $Ca$  (inset, photograph of the free surface deformation).

illuminated polyamide beads (diameter,  $93 \mu\text{m}$ ) dispersed in the oil, and images of the beads were captured after every flapping cycle using a digital SLR camera with  $3072 \times 2048$  pixels per image. The displacement field per flapping cycle was calculated from sequential images using the MatPIV toolbox for MATLAB.

The experimental results are presented in Figs. 4(b) and 4(c). When the surface is free to deform, the reciprocal flapping motion induces a net flow. An example of the vorticity contours (top right is positive vorticity) and flow field over one flapping cycle is displayed in Fig. 4(b): the net flow is induced along the flapper, away from the free surface; when the free surface is replaced by a solid lid, this flow disappears. Measurements of the kinetic energy in the flow (integrated over the whole system) are shown in Fig. 4(c) (nondimensionalized by flapper length and flapping frequency). When the surface is solid (hollow symbols), no flow occurs on average, whereas when the surface is free to deform, the average flow possesses finite kinetic energy (solid symbols), demonstrating that reciprocal actuation near a soft surface can be used to escape the constraints of the scallop theorem.

In summary, we have shown that soft interfaces allow propulsion driven by reciprocal motion. This new strategy for low Reynolds number swimming means not only that primitive swimming methods become effective near a soft interface, but more generally that the usually neglected time-reversible component of all swimmers (including biological organisms and appendages) can generate non-trivial flows and propulsive forces in such settings. The symmetry breaking arises from the normal stress boundary condition: changing the sign of the forcing by a reciprocal swimmer changes the sign of the interfacial normal stresses, thereby changing the interface curvature, and its shape. The strategy is relevant for sufficiently small systems. Moreover, for swimmers of size  $L$  at a distance  $h$  from a surface, the swimming efficiency is expected to scale as  $\mathcal{E} \sim (L/h)^n$  ( $n > 1$ ) and will therefore be most efficient for confined geometries where  $L \sim h$ , for ex-

ample, for the motion of swimmers in thin films and membranes, or near surfaces. Similar results are expected for the dual problem of generating feeding currents from reciprocal forcing. Possible extensions of this work include investigating surface-induced reorientation, rotational swimming, and a closer examination of cases in which surface deformations are large. Together with the current work, this would provide a comprehensive framework for understanding the consequences of soft interfaces on locomotion and transport on small scales.

We thank Denis Bartolo for useful discussions. This work was funded by the NSF (Grant No. CTS-0624830).

\*Corresponding author.  
elauga@ucsd.edu

- [1] E. M. Purcell, *Am. J. Phys.* **45**, 3 (1977).
- [2] J. Lighthill, *SIAM Rev.* **18**, 161 (1976).
- [3] D. Bray, *Cell Movements* (Garland Publishing, New York, 2000).
- [4] R. Dreyfus, J. Baudry, M. L. Roper, M. Fermigier, H. A. Stone, and J. Bibette, *Nature (London)* **437**, 862 (2005).
- [5] C. Berdan and L. G. Leal, *J. Colloid Interface Sci.* **87**, 62 (1982).
- [6] L. G. Leal and S. H. Lee, *Adv. Colloid Interface Sci.* **17**, 61 (1982).
- [7] J. Beaucourt, T. Biben, and C. Misbah, *Europhys. Lett.* **67**, 676 (2004).
- [8] J. M. Skotheim and L. Mahadevan, *Phys. Rev. Lett.* **92**, 245509 (2004).
- [9] L. G. Leal, *Annu. Rev. Fluid Mech.* **12**, 435 (1980).
- [10] I. Cantat and C. Misbah, *Phys. Rev. Lett.* **83**, 880 (1999).
- [11] U. Seifert, *Phys. Rev. Lett.* **83**, 876 (1999).
- [12] U. S. Agarwal, A. Dutta, and R. A. Mashelkar, *Chem. Eng. Sci.* **49**, 1693 (1994).
- [13] G. K. Batchelor, *J. Fluid Mech.* **41**, 545 (1970).
- [14] T. J. Pedley and J. O. Kessler, *Annu. Rev. Fluid Mech.* **24**, 313 (1992).
- [15] J. R. Blake and A. T. Chwang, *J. Eng. Math.* **8**, 23 (1974).
- [16] The linearization around  $h_0$  is valid when  $Mp_0/\omega h_0 \ll 1$  and  $p_0/\eta h_0^3 \omega \ll 1$ ; the quasisteady approximation for the surface deformation is valid for  $\omega \ll \eta/\rho h_0^2$ .
- [17] Interestingly, for real spermatozoa, the swimming speed is only a fraction of the actuation speed of its flagellum (swimming at about  $100\text{--}200 \mu\text{m/s}$  with a  $30\text{--}60 \mu\text{m}$ -long flagellum oscillating at  $30\text{--}50 \text{Hz}$ ); hence, even for weakly confined systems, the effect from soft swimming could be comparable to the “natural” swimming speed.
- [18] For gravity to be irrelevant, the length scales should be small enough for the appropriate Bond numbers to be small; this is usually satisfied in biologically relevant situations where density differences are negligible.
- [19] S. S. Suarez and A. A. Pacey, *Human Reprod. Update* **12**, 23 (2006).
- [20] D. P. Wolf, L. Blasco, M. A. Khan, and M. Litt, *Fertility Sterility* **28**, 41 (1977).
- [21] D. Boal, *Mechanics of the Cell* (Cambridge University Press, Cambridge, U.K., 2002).